

Dissociation of a heavy quarkonium in quark–gluon plasma

Sidi C. Benzahra^{a,*}, Benjamin F. Bayman^b

^a Department of Physics, California Polytechnic State University, San Luis Obispo, CA 93407, USA

^b School of Physics and Astronomy, University of Minnesota, Minneapolis, MN 55455, USA

Received 21 April 2005

Available online 28 September 2005

Abstract

In this work we calculate the dissociation of heavy mesons such as the Υ due to absorption of a thermal gluon in a quark–gluon plasma. We also calculate the dissociation of heavy mesons due to the effect of color charge screening. The lifetime of quarkonium moving with velocity v through a quark–gluon plasma at temperature T is computed. An explicit, configuration–space potential is found for the screened interaction between the quarks constituting the meson. This potential is non-spherical, but axially symmetric about the direction of v . We solve the Schrödinger equation for the relative motion of the quarks in this potential, and use the bound-state wavefunction as the initial state for the dissociation of the meson. The meson lifetime is thus determined as a function of v and T , and conclusions are drawn concerning the possibility of detection of the meson in a high-energy heavy-nucleus collision.

© 2005 Elsevier B.V. All rights reserved.

Keywords: High-energy physics; Quark–gluon plasma; High density; QCD; Quantum chromodynamics

1. Introduction

Calculating the lifetime of quarkonium in a medium of quarks and gluons has much significance in understanding quark–gluon plasma, because it is important to know the lifetime of the Υ compared to the lifetime of the quark–gluon plasma. Since the Υ is imbedded within the plasma, the lifetime of the quark–gluon plasma will have an effect on the lifetime of the Υ . If the lifetime of the quark–gluon plasma is greater than the lifetime of the Υ in the quark–gluon plasma, one would think that there was probably a suppression of Υ 's due to the effect of screening or due to the effect of collision with gluons. This is one such example where calculating the lifetime of the Υ in quark–gluon plasma is indispensable. In fact, many claim that suppression of J/ψ in heavy-ion collision could be a signature of quark–gluon plasma.

There is a relationship between the inverse screening length, m_g ; the number of flavors in the quark–gluon plasma, N_f ; and the temperature of the quark–gluon plasma, T . If we increase the temperature of the quark–gluon plasma, the quarks and the gluons will become very active and some of them will get in between the quark and the antiquark of the meson and cause screening. Thus, the screening increases with the temperature, and the quark and the antiquark can barely “feel” each other. This relationship can be algebraically expressed [1] in the following equation

$$m_g^2 = \frac{1}{3} g^2 \left(N + \frac{N_f}{2} \right) T^2, \quad (1)$$

where $N = 3$ from the color SU ($N = 3$) group, g is the dimensional coupling constant of the field strength, $F_a^{\mu\nu} = \partial^\mu A_a^\nu - \partial^\nu A_a^\mu - gf_{abc} A_b^\mu A_c^\nu$, and $N_f = 3$ is the number of light flavors in the quark–gluon plasma, which are the up, the down, and the strange quarks. We will also use the temperature-dependent running coupling constant of QCD, which is given by [1,2]

* Corresponding author. Tel.: +1 805 756 1696.

E-mail address: sbenzahr@calpoly.edu (S.C. Benzahra).

$$\frac{g^2}{4\pi} = \frac{12\pi}{(11N - 2N_f)\ln(T^2/\Lambda^2)}. \quad (2)$$

This equation explicitly displays asymptotic freedom: $g^2 \rightarrow 0$ as $T \rightarrow \infty$. We notice that there is no intrinsic coupling “constant” on the right-hand side of this equation. The only free parameter of the theory on the right-hand side of this equation is the QCD energy scale, Λ , whose numerical value is dependent on the gauge and on the renormalization scheme chosen. If we choose the QCD energy scale to be $\Lambda = 50$ MeV [1], $N_f = 3$, and $N = 3$ we get

$$m_\varrho = \frac{2\pi T}{\sqrt{3}\ln(T/50)}. \quad (3)$$

There has been an interest in computing the leading correction to Eq. (1) [3]. It is known that this correction cannot be computed perturbatively in non-Abelian gauge [4]. The $O(g^2T)$ correction to the inverse screening length receives contributions from fundamentally non-perturbative physics associated with the interactions, at high temperature, of magnetic gluons with momenta of order g^2T [5].

2. Screened potential

In this section, we study the v -dependence of the bound state of the upsilon because the quark–quark interaction potential calculated by Chu and Matsui [6], and described below, depends upon the velocity of the di-quark system relative to the plasma. We concentrate on the upsilon because in an experiment that produces a very high temperature quark–gluon plasma, the J/ψ will break down at a faster rate compared to the upsilon and only a few of them will survive. This makes it hard for the experimentalist to detect the J/ψ in order to confirm that a quark–gluon plasma had materialized. On the other hand, the upsilon will survive the high-energy density or the high temperature and become easy to detect. Moreover, the upsilon meson is small in size compared to the J/ψ so it needs a higher-density plasma for it to dissociate.

The interaction, in \vec{k} space, of a heavy quark and its antiquark in a moving quark–gluon plasma, was calculated by Chu and Matsui. Their results can be summarized as follows:

$$V(\vec{r}) = \frac{1}{2} \left[QA_\varrho^0(-\vec{r}) + \bar{Q}A_\varrho^0(\vec{r}) \right]. \quad (4)$$

Our goal here is to use this potential to study the stability of the upsilon meson in a quark–gluon plasma, not to repeat the work that Chu and Matsui did in constructing this potential. We did not discuss the physics behind this potential, because this had already been done by Chu and Matsui. Q and \bar{Q} are the color charges of the quark and antiquark, and $A_\varrho^0(\vec{r})$ is the Fourier transform of:

$$\tilde{A}^0(\omega, \vec{k}) = 2\pi Q \delta(\omega) \left[\frac{1 - \gamma^2(1 - \zeta^2)}{\mathbf{k}^2 \epsilon_T(\mathbf{k})} + \frac{\gamma^2(1 - \zeta^2)}{\mathbf{k}^2 \epsilon_L(\mathbf{k})} \right], \quad (5)$$

where

$$\epsilon_T(\mathbf{k}) = 1 + \frac{m_\varrho^2}{\mathbf{k}^2} \phi_T(\zeta); \quad \epsilon_L(\mathbf{k}) = 1 + \frac{m_\varrho^2}{\mathbf{k}^2} \phi_L(\zeta) \quad (6)$$

are the transverse and longitudinal “dielectric constants.” The ϕ_T and ϕ_L are complex functions

$$\Phi_T(\zeta) = \frac{1}{2} \zeta^2 + \frac{1}{4} (1 - \zeta^2) \left[\zeta \ln \left[\frac{1 + \zeta}{1 - \zeta} \right] - i\pi \zeta \theta(1 - \zeta) \right], \quad (7)$$

$$\Phi_L(\zeta) = (1 - \zeta^2) \left[1 - \frac{1}{2} \left[\zeta \ln \left[\frac{1 + \zeta}{1 - \zeta} \right] - i\pi \zeta \theta(1 - \zeta) \right] \right] \quad (8)$$

and ζ is defined by

$$\zeta = \left[\frac{k \cdot u}{\sqrt{(k \cdot u)^2 - k^2}} \right]_{\omega=0} = \frac{v \cos \theta}{\sqrt{1 - v^2 \sin^2 \theta}}, \quad (9)$$

where $u^\mu = \gamma(1, 0, 0, v)$, $k^\mu = (\omega, |\mathbf{k}| \cos \phi \sin \theta, |\mathbf{k}| \sin \phi \sin \theta, |\mathbf{k}| \cos \theta)$, and $k \cdot u \equiv k^\mu u_\mu$. Knowing this, and having the Fourier component of the potential, we can calculate the potential in a cylindrical coordinate system. It takes the form

$$A^0(\vec{r}) = \frac{Qm_\varrho}{4\pi} F(m_\varrho \rho, m_\varrho z). \quad (10)$$

In the Fourier transformation of Eq. (5), both the real and the imaginary parts of the momentum–space potential $\tilde{A}^0(k)$ contribute to the real part of $A^0(\rho, z)$ but no imaginary part appears in the configuration–space potential. The imaginary part of the momentum–space is integrated to generate Bessel function of the first kind.

In order to solve the quark–antiquark Schrödinger equation in \mathbf{r} space, we need an expansion of the interaction potential in the form

$$U(\mathbf{r}) = \sum_{\varrho} u_\varrho(r) P_\varrho(\cos \theta_r) \quad (11)$$

We obtain $U(\mathbf{r})$ by Fourier transforming the \mathbf{k} -space potential given by Chu and Matsui:

$$U(\mathbf{r}) = \frac{1}{2\pi^2} \int d^3\mathbf{k} e^{i\mathbf{k} \cdot \mathbf{r}} V(\mathbf{k}). \quad (12)$$

$V(\mathbf{k})$ is invariant under rotation about \hat{z} , and under reflection across the $\hat{x} - \hat{y}$ plane. Its explicit form is written down below. If we substitute multipole expansion of the plane wave

$$e^{i\mathbf{k}\cdot\mathbf{r}} = \sum_{\ell} i^{\ell} (2\ell+1) j_{\ell}(kr) P_{\ell}(\hat{\mathbf{k}}\cdot\hat{\mathbf{r}}) \\ = 4\pi \sum_{\ell} i^{\ell} j_{\ell}(kr) \sum_{\mu} \left(Y_{\mu}^{\ell}(\hat{\mathbf{k}}) \right)^* Y_{\mu}^{\ell}(\hat{\mathbf{r}})$$

into in Eq. (12), the axial symmetry of $V(\mathbf{k})$ implies that only the $\mu = 0$ terms will survive the $\phi_{\mathbf{k}}$ integration. Comparison with Eq. (11) yields

$$u_{\ell}(r) = i^{\ell} \frac{2}{\pi} (2\ell+1) \int_0^1 dx P_{\ell}(x) \int_0^{\infty} k^2 dk j_{\ell}(kr) V(k, x). \quad (13)$$

The integration variable x in Eq. (13) represents $\cos \theta_{\mathbf{k}}$. Because $V(k, x)$ is an even function of x , only even values of ℓ will occur in the multipole expansion.

The explicit form of $V(k, x)$ is

$$V(k, x) = \frac{k^2 + A}{(k^2 + A)^2 + B^2} (1 - \gamma^2 (1 - \zeta^2)) \\ + \frac{k^2 + C}{(k^2 + C)^2 + D^2} \gamma^2 (1 - \zeta^2), \quad (14)$$

where the x -dependent quantities ζ, A, B, C, D are defined by

$$\zeta \equiv \frac{vx}{\sqrt{1 - v^2(1 - x^2)}},$$

$$A \equiv \frac{1}{2} \zeta^2 + \frac{1}{4} (1 - \zeta^2) \zeta \log \left(\frac{1 + \zeta}{1 - \zeta} \right),$$

$$B \equiv \frac{\pi}{4} (1 - \zeta^2) \zeta,$$

$$C \equiv (1 - \zeta^2) \left(1 - \frac{1}{2} \zeta \log \left(\frac{1 + \zeta}{1 - \zeta} \right) \right),$$

$$D \equiv \frac{\pi}{2} (1 - \zeta^2) \zeta.$$

v is measured in units of c , and k is measured in units of mc/\hbar , the inverse Compton wavelength associated with the screening mass m . The resulting interaction potential is given in units of $(4/3)\alpha mc^2$. The quantities ζ, A, B, C, D defined here are non-negative in the integration region.

The k -integration in Eq. (13) can be done exactly, using the theory of residues. We start with explicit expressions for the even- ℓ spherical Bessel functions:

$$j_{\ell}(kr) = \sum_{m=1,2,\dots,\ell+1} \frac{(\ell+m-1)!}{(\ell-m+1)! 2^{m-1} (m-1)!} \\ \times \frac{a_m^{\ell} \sin(kr) + b_m^{\ell} \cos(kr)}{(kr)^m} \quad (15)$$

with

$$a_m^{\ell} \equiv (-1)^{(\ell+1-m)/2}, \quad b_m^{\ell} \equiv 0 \quad \text{for odd } m$$

$$a_m^{\ell} \equiv 0, \quad b_m^{\ell} \equiv (-1)^{(\ell+s-m)/2} \quad \text{for even } m.$$

Individual terms of the sum in Eq. (15) diverge as $kr \rightarrow 0$, but the entire sum converges as

$$\lim_{kr \rightarrow 0} j_{\ell}(kr) = \frac{(kr)^{\ell}}{(2\ell+1)!!}.$$

For the first term in Eq. (14), we need the integral

$$I_{\ell} \equiv \int_0^{\infty} k^2 dk \frac{k^2 + A}{(k^2 + A)^2 + B^2} j_{\ell}(kr) \quad (\text{even } \ell) \\ = \frac{1}{2} \int_{-\infty}^{\infty} k^2 dk \frac{k^2 + A}{(k^2 + A)^2 + B^2} j_{\ell}(kr) \\ = I_{\ell}^{(+)} + I_{\ell}^{(-)}, \quad (16)$$

with

$$I_{\ell}^{(+)} = \frac{1}{4} \sum_{m=1}^{\ell+1} \frac{(\ell+m-1)! (-ia_m^{\ell} + b_m^{\ell})}{(\ell-m+1)! 2^{m-1} (m-1)! r^m} \\ \times \int_{-\infty}^{\infty} \frac{e^{ikr} (k^2 + A)}{[(k^2 + A)^2 + B^2] k^{m-2}} dk,$$

$$I_{\ell}^{(-)} = \frac{1}{4} \sum_{m=1}^{\ell+1} \frac{(\ell+m-1)! (ia_m^{\ell} + b_m^{\ell})}{(\ell-m+1)! 2^{m-1} (m-1)! r^m} \\ \times \int_{-\infty}^{\infty} \frac{e^{-ikr} (k^2 + A)}{[(k^2 + A)^2 + B^2] k^{m-2}} dk.$$

The contours used for the evaluation of these integrals are shown as xa and xb in Fig. 1. In both cases, the integrand is vanishingly small on the infinite semi-circular parts of the contours. On the real k -axis, and on the semicircle around $k = 0$, the sum of $I_{\ell}^{(+)}$ and $I_{\ell}^{(-)}$ gives us the convergent integrand we need for Eq. (16). Thus we conclude that

$$I_{\ell} = 2\pi i \\ \times [(\text{sum of residues at poles within the contour xa of Fig.1}) \\ - (\text{sum of residues at poles within the contour xb of Fig.1})]. \quad (17)$$

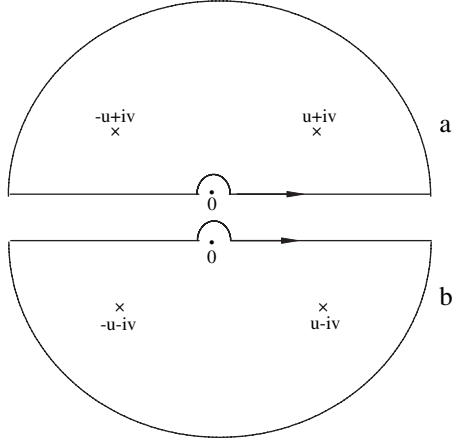


Fig. 1.

We have taken the principle values of the integrals in the equations just above. By integrating around the small semi-circles, centered at the origin, and then allowing the radii of these semi-circles to approach zero, we have evaluated the principal values.

The poles within the contour xa of Fig. 1 are at the zeroes of $(k^2 + A)^2 + B^2$ with positive imaginary parts, i.e. they are at $\pm u + iv$, where

$$u \equiv \sqrt{\frac{\sqrt{A^2 + B^2} - A}{2}}, \quad v \equiv \sqrt{\frac{\sqrt{A^2 + B^2} + A}{2}}.$$

The poles within the contour xb of Fig. 1 are at $\pm u - iv$, and at $k = 0$. The final result is

$$I_\ell = \frac{\pi}{2} e^{-v r} \sum_{m=1}^{\ell+1} \frac{(\ell+m-1)! (a_m^\ell \cos(ur - (m-1)\arctan \frac{v}{u}) - b_m^\ell \sin(ur - (m-1)\arctan \frac{v}{u}))}{(\ell-m+1)! 2^{m-1} (m-1)! (A^2 + B^2)^{(m-1)/4} r^m} + X_\ell, \quad (18)$$

where

$$X_0 \equiv 0,$$

$$X_2 \equiv \frac{\pi}{2} \frac{A}{A^2 + B^2} \frac{3}{r^3},$$

$$X_4 \equiv \frac{\pi}{2} \left[\frac{A}{A^2 + B^2} \frac{15}{2r^3} + \frac{B^2 - A^2}{(A^2 + B^2)^2} \frac{105}{r^5} \right],$$

$$X_6 \equiv \frac{\pi}{2} \left[\frac{A}{A^2 + B^2} \frac{105}{8r^3} + \frac{B^2 - A^2}{(A^2 + B^2)^2} \frac{945}{2r^5} + \frac{A(A^2 - 3B^2)}{(A^2 + B^2)^3} \frac{10395}{r^7} \right],$$

..., etc.

Here X_ℓ represents the contribution to $I_\ell^{(-)}$ of the residue at the $k = 0$ pole.

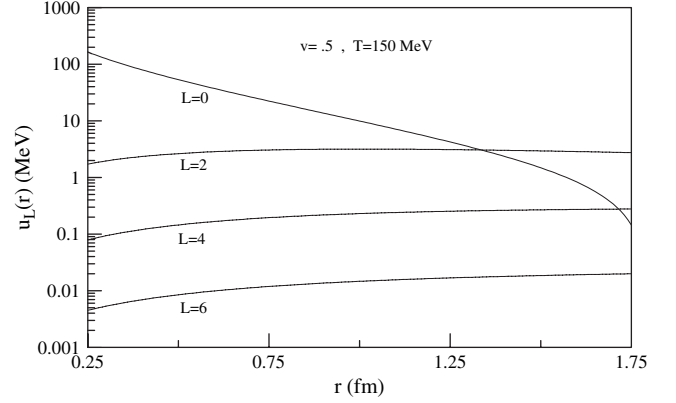


Fig. 2.

The k integral for the second term in Eq. (14) is performed in the same way. Finally, it is necessary to do the x integration in Eq. (13). This must be done numerically. However, since the range is finite ($0 \leq x \leq 1$) and the integrand is smooth, the integrand can be accurately performed with relatively few points. The x -integrations in the results shown below used Simpson's rule, with an x -interval of 0.001 (Fig. 2).

3. Numerical solutions of Schrödinger equation

The binding energy of the quark and the antiquark can also be calculated numerically using the Schrödinger equation. In this case, the non-relativistic Schrödinger equation governing the relative motion of the two quarks is written in the form

$$\left[-\frac{\hbar^2}{2\mu} \nabla^2 + u_0(r) + u_2(r) P_2(\cos \theta) \right] \psi(r, \theta, \phi) = E \psi(r, \theta, \phi), \quad (19)$$

where $\mu = m_Q/2$ is the reduced $Q\bar{Q}$ mass. Looking at the plot of $u_L(r)$ vs. r above, we could see that there is hardly any change for $L = 2, 4, 6$, and so on, thus we could stop at $L = 2$. Because the potential is axially symmetric, the eigenfunctions will be characterized by a definite m -value. However, the spherical symmetry of the potential is destroyed by the $u_2(r) P_2(\cos \theta)$ term, and so the eigenfunctions will not be characterized by a unique value of the total-angular momentum. Thus a solution must be constructed as a linear combination of total-angular-momentum eigenstates:

$$\psi(r, \theta, \phi) = \sum_{\ell} \frac{\phi_{\ell}(r)}{r} Y_{\ell}^m(\theta, \phi). \quad (20)$$

If this expansion is substituted into Eq. (19) the result will be a set of coupled second-order differential equations for the radial functions $\phi_\ell(r)$:

$$\left[\frac{d^2}{dr^2} - \frac{\ell(\ell+1)}{r^2} - \frac{2\mu}{\hbar^2} u_0(r) - k^2 \right] \phi_\ell(r) - \frac{2\mu}{\hbar^2} \sqrt{\frac{4\pi}{5}} u_2(r) \sum_{\ell'} M_{\ell,\ell'} \phi_{\ell'}(r) = 0. \quad (21)$$

Although the ℓ sum in Eq. (21) has, in principle, no upper limit, the sum must be truncated in order to make the calculation finite. In the results to be shown below, the upper limit on ℓ was taken to be 8. In fact, the strength of the coupling potential $u_2(r)$ is small enough so that there was very little mixing of $\ell \neq 0$ components into predominantly $\ell = 0$ eigenfunctions. In Eq. (21) we have introduced the notation

$$E \equiv -\frac{\hbar^2}{2\mu} k^2,$$

$$M_{\ell,\ell'} \equiv \int \sin \theta \, d\theta \, d\phi \, (Y_m^\ell(\theta, \phi))^* Y_0^2(\theta, \phi) Y_m^{\ell'}(\theta, \phi) = \sqrt{\frac{5(2\ell'+1)}{4\pi(2\ell+1)}} (2\ell' \, 0 \, m | \ell \, m) (2\ell' \, 0 \, 0 | \ell \, 0).$$

If we use explicit expressions for the vector-coupling coefficients, we obtain

$$M_{\ell,\ell'} = \frac{1}{2\ell-1} \sqrt{\frac{45(\ell^2-m^2)((\ell-1)^2-m^2)}{16\pi(2\ell-3)(2\ell+1)}} \quad \text{if } \ell = \ell' + 2$$

$$= \sqrt{\frac{5}{4\pi}} \frac{\ell(\ell+1) - 3m^2}{(2\ell-1)(2\ell+3)} \quad \text{if } \ell = \ell'$$

$$= \frac{1}{2\ell'-1} \sqrt{\frac{45(\ell'^2-m^2)((\ell'-1)^2-m^2)}{16\pi(2\ell'-3)(2\ell'+1)}} \quad \text{if } \ell' = \ell + 2.$$

In order to describe bound states of the meson we must find normalizable solutions of the coupled Eq. (21) which are regular at $r = 0$. This defines an eigenvalue condition for k^2 .

A convenient numerical approach to this problem is suggested by the simple special case in which $u_2(r) = 0$. The coupling terms in Eq. (21) vanish, leading to the single equation

$$\left[\frac{d^2}{dr^2} - \frac{\ell(\ell+1)}{r^2} - \frac{2\mu}{\hbar^2} u_0(r) - k^2 \right] \phi_\ell(r) = 0. \quad (22)$$

We choose an arbitrary radius, R , and we guess a value for k^2 . We then find an *interior* solution $\phi_\ell^i(r)$ by numerically integrating Eq. (22) from $r = 0$ to $r = R$, starting at $r = 0$ with the behavior

$$\phi_\ell^i(r) \xrightarrow{r \rightarrow 0} r^{\ell+1}. \quad (23)$$

Then we find an *exterior* solution $\phi_\ell^e(r)$ by numerically integrating Eq. (22) from a very large value of r down to $r = R$, starting at the large value of r with the behavior

$$\phi_\ell^e(r) \xrightarrow{r \rightarrow \infty} h_\ell^1(ikr). \quad (24)$$

The eigenvalue condition on k is that the relative normalizations of the interior and exterior functions can be chosen so that there is no discontinuity in value and slope at $r = R$. This requires that their logarithmic derivatives at $r = R$ be equal, which we can express as the condition

$$\frac{\phi_\ell^e(R) \phi_\ell^{i'}(R)}{\phi_\ell^{e'}(R) \phi_\ell^i(R)} - 1 = 0. \quad (25)$$

k^2 in Eq. (22) is varied until this condition is satisfied. The values of k^2 so obtained are independent of the arbitrarily chosen R . This can be seen by using Eq. (22) to show that

$$0 = \phi_\ell^e \frac{d^2}{dr^2} \phi_\ell^i - \phi_\ell^i \frac{d^2}{dr^2} \phi_\ell^e = \frac{d}{dr} \left[\phi_\ell^e \frac{d}{dr} \phi_\ell^i - \phi_\ell^i \frac{d}{dr} \phi_\ell^e \right], \quad (26)$$

so that $\phi_\ell^e(d/dr)\phi_\ell^i - \phi_\ell^i(d/dr)\phi_\ell^e$ is independent of r , and so if Eq. (25) is true at one value of r , it is true at all r . To generalize this procedure to the full set of coupled Eq. (21), we define sets of interior and exterior functions by

$$a_{\ell,\ell_1}(r) \xrightarrow{r \rightarrow 0} \delta_{\ell,\ell_1} r^{\ell+1}, \quad (27)$$

$$b_{\ell,\ell_2}(r) \xrightarrow{r \rightarrow \infty} \delta_{\ell,\ell_2} h_\ell^1(ikr). \quad (28)$$

We now attempt to choose linear combinations of these interior and exterior functions

$$\phi_\ell^i(r) = \sum_{\ell_1} a_{\ell,\ell_1}(r) \alpha_{\ell_1}, \quad (29)$$

$$\phi_\ell^e(r) = \sum_{\ell_2} b_{\ell,\ell_2}(r) \beta_{\ell_2} \quad (30)$$

in order to achieve continuity of value and derivative at the matching radius $r = R$. This requires that the coefficients α_{ℓ_1} and β_{ℓ_2} satisfy

$$\sum_{\ell_1} a_{\ell,\ell_1}(R) \alpha_{\ell_1} = \sum_{\ell_2} b_{\ell,\ell_2}(R) \beta_{\ell_2}, \quad (31)$$

$$\sum_{\ell_1} a'_{\ell,\ell_1}(R) \alpha_{\ell_1} = \sum_{\ell_2} b'_{\ell,\ell_2}(R) \beta_{\ell_2}. \quad (32)$$

We can express this as a condition on the β_ℓ alone by using Eq. (31) to eliminate α_{ℓ_1} from Eq. (32):

$$\alpha_{\ell_1} = \sum_{\ell_2} [a^{-1}(R)b(R)]_{\ell_1,\ell_2} \beta_{\ell_2}, \quad (33)$$

$$\sum_{\ell_2} \left[b'^{-1}(R) a'(R) a^{-1}(R) b(R) \right]_{\ell_1, \ell_2} \beta_{\ell_2} = \beta_{\ell_1}. \quad (34)$$

The necessary and sufficient condition for a non-trivial solution to Eq. (34) is

$$\det \left[b'^{-1}(R) a'(R) a^{-1}(R) b(R) - \mathbf{1} \right] = 0. \quad (35)$$

This is the multi-channel generalization of Eq. (25). The value of k^2 used in the numerical integration of the coupled Eq. (21) is varied until Eq. (35) is satisfied to an acceptable accuracy. Then Eqs. (33) and (34) determine the α_{ℓ} and β_{ℓ} up to an overall multiplicative factor, which can be obtained from the normalization condition

$$\sum_{\ell} \int_0^R dr \left[\sum_{\ell_1} a_{\ell, \ell_1}(r) \alpha_{\ell_1} \right]^2 + \sum_{\ell} \int_R^{\infty} dr \left[\sum_{\ell_2} b_{\ell, \ell_2}(r) \beta_{\ell_2} \right]^2 = 1. \quad (36)$$

As in the one-channel case, the consistency of the procedure guarantees that the calculated energy eigenvalues and eigenfunctions are independent of the choice of the matching radius.

The numerical integration of the coupled differential equations was performed using the 4th-order Runge–Kutta method with a step-length of 0.01 fm, starting at a minimum radius of 0.001 fm [7]. Although the ℓ sum in Eq. (21) has, in principle, no upper limit, the sum must be truncated in order to make the calculation finite. In the results to be shown below, the upper limit on ℓ was taken to be 8. In fact, the strength of the coupling potential $u_2(r)$ is small enough so that there was very little mixing of $\ell \neq 0$ components into predominantly $\ell = 0$ eigenfunctions.

Here we use [8] $\alpha_s(m_b) = 0.232$, and $m_Q = 4.3$ GeV. Here, we employed a quark mass of 4.3 GeV because our model of the upsilon is one bottom and one anti-bottom quark, and the mass of each of these constituent quarks is 4.3 GeV. This mass of 4.3 GeV is kept constant throughout the paper. In our model relative motion of the constituent quarks is non-relativistic, and so these constituent quarks have constant mass. The mass and the α_s are obtained from QCD sum rules and lattice QCD. But as you can see in Fig. 3, the binding energies are very small. Our study here refers to the binding energy of the upsilon in a hot quark–gluon plasma. The presence of the plasma determines the quark–gluon interaction that we use. The binding energy of the free upsilon is about 800 MeV, but the binding energy decreases when we immerse the upsilon in the quark–gluon plasma.

The ν -dependence of the binding energy in Fig. 3 is a consequence of the ν -dependence of the interaction, which is described in the work of Chu and Matsui [6].

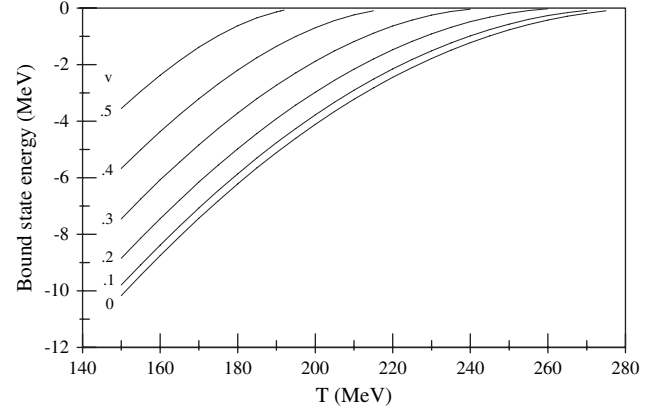


Fig. 3.

4. Dissociation time of a heavy meson due to collision with thermal gluons

Let us introduce the calculation of the dissociation time by asking: what is the rate of photo-ionization if we place a hydrogen atom in a cavity of thermalized photons at temperature T ? The Planck distribution [9] states that the flux of photons, photons/unit area-unit time, in the interval dk around k is

$$\frac{ck^2 dk}{\pi^2 [e^{hkc/T} - 1]}. \quad (37)$$

Let $\sigma(k)$ be the cross-section for photo-emission when the incident photon has momentum k . The rate for this process is

$$R = \int_0^{\infty} \frac{ck^2 \sigma(k)}{\pi^2 [e^{hkc/T} - 1]} dk. \quad (38)$$

According to Gasiorowicz, Quantum Physics, Chapter 24 [10]

$$\sigma(k) = \frac{V p_e e^2}{2\pi \hbar^3 m c^2 k} \int d\Omega \left| \int d^3 r \psi_f^*(\vec{r}) \hat{\epsilon} \cdot \vec{p} e^{ikz} \psi_i(\vec{r}) \right|^2. \quad (39)$$

$\psi_i(\vec{r})$ is normalized wavefunction of the initial bound electron state, p_e is the asymptotic momentum of the outgoing electron [11], and m is its mass.

$$\psi_f(\vec{r}) \xrightarrow{r \rightarrow \infty} \frac{1}{\sqrt{V}} \left[e^{i\vec{k}_e \cdot \vec{r}} + f(\theta', \phi') \frac{e^{-ik_e r}}{r} \right], \quad (40)$$

$$\vec{k}_e = \frac{\vec{p}_e}{\hbar} = k_e [\sin \theta' (\cos \phi' \hat{x} + \sin \phi' \hat{y}) + \cos \theta' \hat{z}].$$

The $d\Omega$ integration is over θ' , ϕ' , the asymptotic direction of the outgoing electron.

Let's now consider the transition from QED to QCD. In QED the electron–photon vertex [9] is associated with matrix element of

$$ig_e \gamma^\mu = i \sqrt{\frac{4\pi e^2}{\hbar c}} \gamma^\mu. \quad (41)$$

In QCD the quark–gluon vertex Eq. [12] is associated with matrix element of

$$-i \frac{g_s}{2} \lambda^\alpha \gamma^\mu = -i \sqrt{\frac{4\pi \alpha_s}{2}} \lambda^\alpha \gamma^\mu. \quad (42)$$

The λ^α is a generator of color SU(3). ($\alpha = 1, 2, \dots, 8$). We are going from a meson (color singlet) to a $Q\bar{Q}$ octet.

$$\langle [\text{octet}]_\alpha | \lambda^\alpha | [\text{singlet}] \rangle = \sqrt{\frac{8}{3}}.$$

Thus

$$i \sqrt{\frac{4\pi e^2}{\hbar c}} \longleftrightarrow -i \sqrt{\frac{4\pi \alpha_s}{2}} \sqrt{\frac{8}{3}},$$

which gives us

$$\frac{e^2}{\hbar c} \longleftrightarrow \frac{2}{3} \alpha_s.$$

The photon flux density is multiplied by 8 to get the total gluon density (8 types of gluons, 8 generators of SU(3)). Moreover, it is necessary to include the fact that the meson moves with speed $v = \beta c$ relative to the plasma, and so it sees a Lorentz-shifted Planck distribution for the gluon momenta. After averaging over the gluon directions, we finally obtain

$$R = \int_0^\infty \frac{8ck^2 \sigma(k)}{\pi^2} \left[\frac{T}{2\gamma\beta\hbar ck} \log \left(\frac{e^{(\hbar ck\gamma/T)(1+\beta)} - 1}{e^{(\hbar ck\gamma/T)(1-\beta)} - 1} \right) - 1 \right] dk \quad (43)$$

and

$$\sigma(k) = \frac{V p_{Q\bar{Q}}^2 \alpha_s}{2\pi \hbar^2 \mu c k} \int d\Omega \left| \int d^3r \psi_f^*(\vec{r}) \hat{\epsilon} \cdot \vec{p} e^{ikz} \psi_i(\vec{r}) \right|^2, \quad (44)$$

where μ is the reduced $Q\bar{Q}$ mass.

Evaluating $\sigma(k)$, Muller [13] replaces e^{ikz} by 1 (long-wavelength approximation) and $\psi_f(\vec{r})$ by $e^{i\vec{k}_Q \cdot \vec{r}}$ (no distortion of outgoing wave) and neglects the connection between k_Q and k . We will make none of these approximations.

Now let's expand the wavefunction

$$\psi_f(\vec{r}) = \frac{4\pi}{\sqrt{V}} \sum_{\ell} i^\ell e^{-i\delta_\ell} \sum_m Y_m^{\ell*}(\theta', \phi') Y_m^\ell(\theta, \phi) \frac{W_\ell(r)}{r}, \quad (45)$$

$$\begin{aligned} \hat{\epsilon} \cdot \vec{p} e^{ikz} \psi_i(\vec{r}) &= \frac{\hbar}{i} \hat{\epsilon} \cdot \vec{\nabla} e^{ikz} \psi_i(r) \\ &= \frac{\hbar}{i} e^{ikz} \hat{\epsilon} \cdot \vec{\nabla} \psi_i(r) \\ &= \frac{\hbar}{i} e^{ikz} \hat{\epsilon} \cdot \hat{r} \psi_i'(r). \end{aligned} \quad (46)$$

The three equalities just above are satisfied since $\hat{\epsilon} \cdot \hat{z} = 0$ (gluon has transverse polarization) and since $\psi_i(\vec{r}) \approx \psi_i(r)$ (spherically symmetric ground state). Let

$$I(\vec{k}_Q) = \int d^3r \psi_f^*(\vec{r}) \hat{\epsilon} \cdot \vec{p} e^{ikz} \psi_i(\vec{r}), \quad (47)$$

which is the same as

$$\begin{aligned} I(\vec{k}_Q) &= \frac{\hbar}{i} \frac{4\pi}{\sqrt{V}} \sum_{\ell, m} i^{-\ell} e^{i\delta_\ell} Y_m^\ell(\theta', \phi') \\ &\quad \times \int d^3r Y_m^{\ell*}(\theta, \phi) \frac{W_\ell(r)}{r} \hat{\epsilon} \cdot \hat{r} e^{ikz} \psi_i'(r), \end{aligned} \quad (48)$$

where

$$\begin{aligned} \hat{\epsilon} \cdot \hat{r} &= \epsilon_x \sin \theta \cos \phi + \epsilon_y \sin \theta \sin \phi \\ &= \sqrt{\frac{2\pi}{3}} [-(\epsilon_x - i\epsilon_y) Y_1^1(\theta, \phi) + (\epsilon_x + i\epsilon_y) Y_{-1}^1(\theta, \phi)]. \end{aligned}$$

Now we use the relation

$$Y_{\pm 1}^1(\theta, \phi) e^{ikz} = \sqrt{\frac{3}{2}} \sum_{\ell} i^{\ell-1} \sqrt{\ell(2\ell+1)(\ell+1)} \frac{j_\ell(kr)}{kr} Y_{\pm 1}^\ell(\theta, \phi). \quad (49)$$

Substituting Eq. (49) in Eq. (48), we get

$$\begin{aligned} I(\vec{k}_Q) &= \frac{4\pi^{3/2} \hbar}{\sqrt{V} k} \sum_{\ell=1}^{L_{\max}} e^{i\delta_\ell} \sqrt{\ell(2\ell+1)(\ell+1)} \\ &\quad \times [(\epsilon_x - i\epsilon_y) Y_1^1(\theta', \phi') - (\epsilon_x + i\epsilon_y) Y_{-1}^1(\theta', \phi')] \\ &\quad \times \int_0^\infty dr j_\ell(kr) W_\ell(r) \psi_i'(r). \end{aligned} \quad (50)$$

When we integrate over θ' and ϕ' we use the orthonormality of the spherical harmonics:

$$\int Y_{m_1}^{\ell_1*}(\theta', \phi') Y_{m_2}^{\ell_2}(\theta', \phi') d\Omega = \delta_{\ell_1, \ell_2} \delta_{m_1, m_2}. \quad (51)$$

Then the coherent sum over ℓ in $I(\vec{k}_Q)$ becomes an incoherent ℓ sum in $\sigma(k)$

$$\sigma(k) = \frac{32}{3} \pi^2 \alpha_s \frac{\hbar c}{m_Q c^2} \frac{k_Q}{k^3} \sum_{\ell=1}^{L_{\max}} \ell(2\ell+1)(\ell+1) \times \left| \int_0^{\infty} dr j_{\ell}(kr) W_{\ell}(r) \psi'_{\ell}(r) \right|^2. \quad (52)$$

Eq. (52) is inserted into Eq. (43), and the integration over k is carried out numerically. Fig. 4 shows the plot of calculated lifetime $\tau = (1/R)$ as a function of T .

Fig. 4 shows that the velocity of the meson in quark–gluon plasma plays a major role in dissociating the meson. If the meson is moving at greater velocity, it needs less temperature to break itself down than if it is moving at lower velocity. Interesting results are also shown in this graph. If we fix the velocity of the meson and study only the relationship between the lifetime of the meson and the temperature of the quark–gluon plasma where the meson is imbedded, we observe that the lifetime of the meson increases with the temperature. When we increase the temperature we are also increasing the flux of gluons in the quark–gluon plasma. But in the k region where the flux is significant, the cross-section, $\sigma(k)$, of the collision of gluon with the quarks of meson is a decreasing function of k . When k increases beyond about 0.5 fm^{-1} , and k_{minimum}^i exceeds 2 fm^{-1} , it will be difficult to find, in the initial meson wavefunction, components with k_Q^i big enough to satisfy both conservation of momentum and conservation of energy. This $\sigma(k)$ falls as k increases, in the vicinity of 0.5 fm^{-1} . Furthermore, as T increases, the screening between Q and \bar{Q} in the meson becomes more effective. There is less binding, the size of the relative $Q\bar{Q}$ wavefunction increases, and the presence of large k_Q^i in the initial state diminishes. This makes it more difficult to satisfy both the conservation of momentum and the conservation of energy as T increases, and causes $\sigma(k)$, in the k region where the flux is significant, to be a decreasing function of T . In our model we are looking at the absorption of a gluon by a quark; in a different model one can also consider the case $Q + g \rightarrow \bar{Q} + g$ which might not make the lifetime increase with temperature. We are here concerned

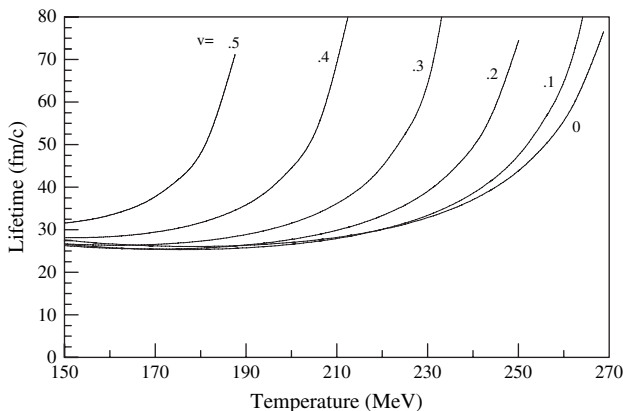


Fig. 4.

with the binding energy of an upsilon immersed in a quark–gluon plasma, and stability with respect to dissociation due to gluon absorption. We agree that another dissociation mechanism would involve collision (not absorption) of a gluon and a quark. That could be the subject of another investigation.

When T decreases below $T = 170 \text{ MeV}$, the disintegration rate decreases because of falling gluon flux. As T increases above $T = 170 \text{ MeV}$, the disintegration rate decreases because of falling $\sigma(k)$. The maximum disintegration rate at $T \approx 170 \text{ MeV}$ leads to a minimum lifetime of $\sim 27.5 \text{ fm/c}$. No minimum with respect to T was predicted by Muller [10] since he did not take into account both momentum and energy conservation. The expected lifetime of the quark–gluon plasma is $10\text{--}20 \text{ fm/c}$, which is appreciably shorter than our minimum meson-disintegration lifetime of 27.5 fm/c . Thus our conclusion is that the plasma will cease to exist before a significant fraction of the mesons will have been disintegrated by gluon impact. Therefore, this process will not have an appreciable effect on the number of mesons observed.

5. Relation of results to experiment

Recent experiments [14] at the CERN SPS have shown a large suppression of J/ψ production in central Pb + Pb collisions. Following the original idea of Matsui and Satz [15] that J/ψ would be dissociated in a quark–gluon plasma due to color screening, the observed J/ψ suppression has been suggested as an evidence for the formation of the quark–gluon plasma in these collisions [16–18].

Since the upsilon meson states in a quark–gluon plasma are also sensitive to the color screening effect [15,19,20], the study of the upsilon meson suppression in high-energy heavy-ion collisions can be used as a signature for the quark–gluon plasma as well. Because the binding energy of Υ is larger than that of J/ψ , the critical energy density at which an upsilon meson is dissociated in the quark–gluon plasma is also higher [21]. One therefore expects to see the effects of the quark–gluon plasma on the production of the upsilon meson only in ultra-relativistic heavy-ion collisions such as at the RHIC and the LHC. As in the case of J/ψ , one needs to understand the effects of the upsilon meson absorption in hadronic matter in order to use its suppression as a signal for the quark–gluon plasma in heavy-ion collisions.

In the study of screening, if we detect an upsilon meson in an experiment which produces a quark–gluon plasma of a temperature higher than 275 MeV , we know that this upsilon meson did not pass through this quark–gluon plasma, since we have found that the highest temperature at which the upsilon meson is bound is about 275 MeV , at $v = 0$. If the meson was moving it would even have less of a chance to survive this temperature, since we have found the binding energy of the meson to decrease with the velocity.

In the study of absorption of a thermal gluon by a quark or antiquark, one could say that the upsilon meson has survived because the quark–gluon plasma has died out before it could dissociate it, since we have calculated the lifetime of the

meson to be somewhat greater than the lifetime of the quark–gluon plasma.

In an experiment which produces a very high temperature quark–gluon plasma, the J/ψ will break down at a faster rate compared to the Υ and only a few of them will survive. This makes it hard for the experimentalist to detect the J/ψ in order to confirm that a quark–gluon plasma had materialized. On the other hand, the Υ will survive the high-energy density or the high temperature and become easy to detect. Moreover, the Υ meson is small in size compared to the J/ψ so it needs a higher-density plasma for it to dissociate.

Acknowledgements

The authors would like to thank Joseph I. Kapusta for his very useful help.

Part of this work is supported by the U.S. Department of Energy under contract DE-AC03-76SF00098, and grant DE-FG02-87ER40328.

References

- [1] J.I. Kapusta, Finite Temperature Field Theory, Cambridge University Press, Cambridge, 1989.
- [2] J.I. Kapusta, Phys. Rev. D 46 (10) (1992) 4749.
- [3] K. Kajantie, J.I. Kapusta, Phys. Lett. B 110 (1982) 299.
- [4] S. Nadkarni, Phys. Rev. D 22 (1986) 3738; A.K. Rebhan, Phys. Rev. D 48 (1993) R3967.
- [5] P. Arnold, L.G. Yaffe, Phys. Rev. D 52 (1995) 7208–7219.
- [6] M.C. Chu, T. Matsui, Phys. Rev. D 39 (1989) 1892.
- [7] William H. Press, Saul A. Teukolsky, William T. Vetterling, Brian P. Flannery, Numerical Recipes in Fortran 97, second ed. Cambridge University Press, 1992 (Chapter 16).
- [8] Matthias Jamin, Antonio Pich, Nucl. Phys. B 507 (1997) 334–352.
- [9] F. Reif, Fundamentals of Statistical and Thermal Physics, McGraw-Hill, Inc., Singapore, 1965.
- [10] S. Gasiorowicz, Quantum Mechanics, second ed. John Wiley and Sons, Inc., 1996.
- [11] G. Breit, H.A. Bette, Phys. Rev. 93 (1954) 888.
- [12] F. Halzen, A. Martin, Quarks and Leptons, John Wiley and Sons, Inc., 1984.
- [13] B. Muller, preprint nuc-th/9806023, v2, in press.
- [14] M. Gonin, et al. The NA50 Collaboration, Nucl. Phys. A 610 (1996) 404c; M.C. Abreu, et al. The NA50 Collaboration, Phys. Lett. B 450 (1999) 456.
- [15] T. Matsui, H. Satz, Phys. Lett. B 178 (1986) 416.
- [16] J.-P. Blaizot, J.-Y. Ollitrault, Phys. Rev. Lett. 77 (1996) 1703.
- [17] C.-Y. Wong, Nucl. Phys. A 630 (1998) 487.
- [18] D. Kharzeev, M. Nardi, H. Satz, Phys. Lett. B 405 (1997) 14 D. Kharzeev, C. Lourenco, M. Nardi and H. Satz, Z.
- [19] S.C. Benzahra, Phys. Rev. C 61 (2000) 064906.
- [20] For recent reviews, see, e.g., R. Vogt, Phys. Rep. 310 (1999) 197; H. Satz, Rep. Prog. Phys. 63 (2000) 1511.
- [21] F. Karsch, M.T. Mehr, H. Satz, Z. Phys. C 37 (1988) 617.